Legendre-based node-dependent kinematics shell models for the global–local analysis of homogeneous and layered structures

(Article begins on next page)

26 September 2024

Legendre-based node-dependent kinematics shell models for the global–local analysis of homogeneous and layered structures

E. Carrera[1], A. Pagani [*,2], D. Scano[3]

Mul² Group, Department of Mechanical and Aerospace Engineering, Politecnico di Torino Corso Duca degli Abruzzi 24, 10129 Torino, Italy

ARTICLE INFO

ABSTRACT

The present work demonstrates the use of the node-dependent kinematics method to derive and compare several two-dimensional shell theories. The three dimensional displacement field is expressed in terms of generalized coordinates, which are subsequently expanded along the shell thickness using arbitrary functions. The in-plane unknowns, are then discretized through classical finite element approximation. Based on the Carrera Unified Formulation, the proposed method combines in a unique manner the theory of structures and the finite element method; thickness interpolation functions are defined node-wise. As a consequence, the resulting finite element model represents diverse approximation theories at each single node. In this work Taylor-based kinematics (including the Murakami Zig-Zag function) and Legendre-type nodal kinematics are incorporated at the element level without adopting mathematical artifices leading to the global–local strategy, where refined theories are selectively employed in specific areas, while maintaining acceptable computational costs. Numerical cases from the existing literature are employed to establish the effectiveness of node-dependent models in bridging a locally refined theories to global kinematics when local effects need to be considered. The analyses focus on localized loads for both homogeneous and multi-layered structures.

1. Introduction

Shell structures play a significant role in a wide range of engineering applications due to their efficient load-carrying capabilities. However, the continuous development of new structural materials, including composite layered materials, has led to increasingly complex structural designs that demand intensive analysis. Nonetheless, addressing these challenges often results in a substantial increase in computational costs.

Over the past few decades, numerous shell models have been introduced. The initial and less computationally intensive two-dimensional (2D) model is known as Thin Shell Theory (TPT), which is rooted in Kirchhoff's theory (Kirchhoff, 1850). Kirchhoff's hypothesis assumes that the section of the shell remains orthogonal to the reference surface during deformation. Consequently, out-of-plane components of the strains are disregarded. The extension for the composite structures was proposed Classical Lamination Theory (CLT) in Reissner and Stavsky (1961). The First Shear Deformation Theory (FSDT) was developed to account for transverse shear deformation. It originated from the works of Reissner (1945) and Mindlin (1951) and was subsequently employed to propose various structural models within the context of

the Finite Element Method (FEM). Notable contributions include the works of Pryor and Barker (1971), Noor and Mathers (1977) and Panda and Natarajan (1979), as well as Parisch (1979). Classical models, based on these theories, continue to be used in commercial software today. Although, the classical theories work well for thin and isotropic shells and do not satisfy the compatibility requirements, they are still used in the commercial codes for their simplicity and a relatively low computational cost, see Argyris (1966).

Because classical models are not well-suited for accurately analyzing thick and/or composite materials, Higher-Order Theories (HOT) have been introduced over the years. Notable among these are the refined models proposed by Reddy (1984). Carrera conducted a historical review of zig-zag theories, with a specific emphasis on the plate/shell formulation, as detailed in Carrera (2003). Additionally, in Carrera (2001), the same author presented advanced models based on Reissner's Mixed Variational Theorem (RMVT). In these theories, higher-order expansions of the displacement fields are assumed along the laminae of the composite structure and were presented by Kant et al. (1982) and Kant and Kommineni (1994). Reddy (1997) employed refined models for both plates and shell structures. Kulikov

* Corresponding author.
  E-mail addresses: erasmo.carrera@polito.it (E. Carrera), alfonso.pagani@polito.it (A. Pagani), daniele.scano@polito.it (D. Scano).
[1] Professor of Aeronautics and Astronautics.
[2] Associate Professor.
[3] PhD Student.

and Carrera (2008) proposed higher-order shell models by using interpolation surfaces. In contrast, Zig-zag functions are introduced into classical or higher-order theories. These functions are piecewise and designed to meet the mechanical requirements of laminated materials. Numerous finite element (FE) implementations have been developed based on these methods. For instance, see the works of Murakami (1986), Aitharaju (1999), and Cho and Averill (2000). Additionally, Kumar et al. (2013) proposed a shell element that incorporates higher-order Zig-Zag models. Nguyen et al. (2015) implemented a Zig-Zag theory to analyze viscoelastic laminated composite plate. Cho and Oh (2004) studied smart materials by using a fully coupled thermo-electro–mechanical formulation. Finally, Carrera (1996) and Carrera and Demasi (2002) introduced the Carrera Unified Formulation (CUF) for plate and shell theories. This method allows the flexibility to select both the structural theory and the shape functions according to specific requirements.

In most of the previously discussed papers, an Equivalent Single Layer (ESL) approach for modeling composite structures is commonly adopted. ESL models feature variables that are independent of the number of mathematical domains. On the contrary, the Layer Wise (LW) approach is employed when precise and detailed analyses are needed, particularly for accurate shear stress determination. In LW models, each layer is described by distinct sets of variables. Numerous authors have successfully integrated LW theories with finite element (FE) formulations. Notable works include those by Rammerstorfer et al. (1992), Reddy (1993), Mawenya and Davies (1974), Noor and Burton (1990), and Carrera (1998). The latter adopted the CUF framework. It is worth noting that the LW approach necessitates a more computationally intensive effort due to the inclusion of a greater number of degrees of freedom in the models.

Although the previously mentioned models lead to increased accuracy, they simultaneously lead to a significant increase in computational costs. In cases involving complex local phenomena such as delamination (Airoldi et al., 2015), cracks (Haryadi et al., 1998), or local buckling (Kubiak et al., 2016), a more detailed local solution is often required. To manage and control these computational costs, several approaches have been developed in recent decades. For instance, one commonly employed method involves the use of refined models in regions where higher-order effects need to be analyzed, as described by Reddy (1989). In contrast, the remainder of the structure is discretized using lower fidelity models. By doing so, the total number of degrees of freedom can be reduced with only a minor decrease in solution accuracy. Implementing global–local models, however, is not a trivial task. Over the past few decades, scholars have proposed various methods for integrating different structural theories in the same mathematical model. For a comprehensive overview of these approaches, interested readers are referred to the review by Noor (1986). In his work, Noor summarized the criteria for developing a coherent global–local method; *[...]The effective implementation of this approach requires the following:*

1. *systematic procedure for generating the hierarchy of mathematical models[...],*
2. *criteria for the adaptive refinement of the mathematical model, and*
3. *treatment of the interfaces between the different regions.*

When two domains described by different models must be connected, several issues come into play. Most notably, the compatibility of displacements between these domains must be ensured. For instance, Fish et al. (1996) introduced a multi-grid method that relies on an iterative algorithm to share information between coarse and fine meshes. In the context of global–local analysis, researchers have proposed methods involving the use of Lagrange multipliers, as demonstrated by Prager (1968). In this context, Park and Felippa (2000) utilized a continuum-based variational principle to formulate discrete governing equations for partitioned structural systems. Additionally, Aminpour et al. (1995) and Ransom (2001) employed a spline method to establish connections between two domains discretized by different finite elements.

Lastly, Blanco et al. (2008, 2011) employed an eXtended Variational Formulation (XVF) by adopting the Lagrange multiplier approach. An alternative approach for ensuring compatibility between two zones is to introduce an overlapping zone. Dhia (1998) and Dhia and Rateau (2005) initially proposed the Arlequin method, which utilizes Lagrange multipliers. This method was subsequently implemented in the context of the CUF for plate and beam models by Biscani et al. (2012) and Carrera et al. (2013), respectively.

This work demonstrates the capabilities of the Node-Dependent Kinematics (NDK) approach, as implemented in the CUF framework for the shell formulation. It employs combinations of Legendre-Legendre, Legendre-Taylor, and Legendre-Taylor with Zig-Zag functions. Due to the hierarchical nature of CUF, it is possible to select the desired structural theory for each element node without resorting to additional mathematical techniques. Specifically, for a 2D problem, the expansion functions change across the shell mid-plane. Within the Finite Element Method (FEM), there are no restrictions to combining different structural theories. This flexibility allows for the arbitrary use of low- to higher-order theories. The NDK method was initially introduced by Carrera and Zappino (2017) for linear static analysis within the beam formulation. This approach was subsequently extended to the plate formulation for multilayered structures by Zappino et al. (2017), who proposed FE models using Lagrange and Taylor Zig-Zag functions. On the other hand, Carrera et al. (2017) employed Legendre and Taylor expansions. Carrera et al. (2018) also introduced the NDK method for electro-mechanical problems in the shell formulation.

Even though the expansion along the thickness is formally the same for both plates and shells, the problems are intrinsically different, from both practical and mathematical perspectives. In fact, the shell formulation considers finite curvatures. This permits to explore different types of structures, while the application of plate formulation is restricted to the plane cases. Thus, the shell formulation allows to describe exactly the geometries of the structures. In the open literature, the shell and the plate formulations are usually studied in an independent manner.

Finally, it is worth noting that FE analysis can suffer from significant stiffening when dealing with thin structures. The plate elements are affected by the shear locking, while the membrane locking must be considered in the shell elements as well. The first phenomenon is related to the incapacity of the finite elements to calculate the bending deformation, and the strain energy is erroneously absorbed by the shear mode. Physically, the transverse shear energy tends to zero when the structures become thinner. On the other hand, the membrane locking occurs when the stretching of the mid-plane is incorrectly calculated during a bending deformation. In this way, the membrane energy overcomes the bending energy. To address these numerical issues, the present paper employs the Mixed Interpolation of Tensorial Components (MITC) method (Bathe and Dvorkin, 1986; Bucalém and Bathe, 1993). The MITC integration method has been integrated into the shell formulation within the CUF framework. It is beyond this work to fully demonstrate the application of MITC. More details can be found in the work of Cinefra and Carrera (2013).

This paper is organized as follows: Section 2 provides a review of the Hierarchical Legendre Expansions for the shell formulation. Section 3 offers an overview of the modeling approaches for composite structures. Section 4 covers the shell formulation within the CUF. This section also introduces the Node-Dependent Kinematics method and presents the governing equations. It concludes with an illustration of the assembly of the stiffness matrix. Section 5 presents the results obtained for a doubly-pinched cylinder and a composite shell. Finally, in Section 6, the paper summarizes the most significant conclusions.

2. Two-dimensional models based on Hierarchical Legendre polynomials

In the present work, Hierarchical Legendre Expansion (HLE) utilizes Legendre polynomials to formulate structural theories. The theoretical
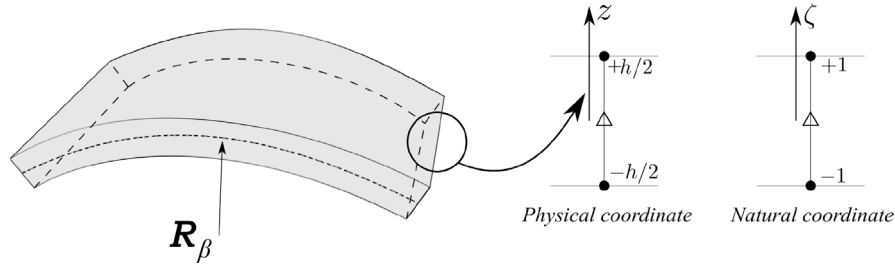
Fig. 1. Hierarchical Legendre Expansions for shells. Definition of vertexes ● and edges △.
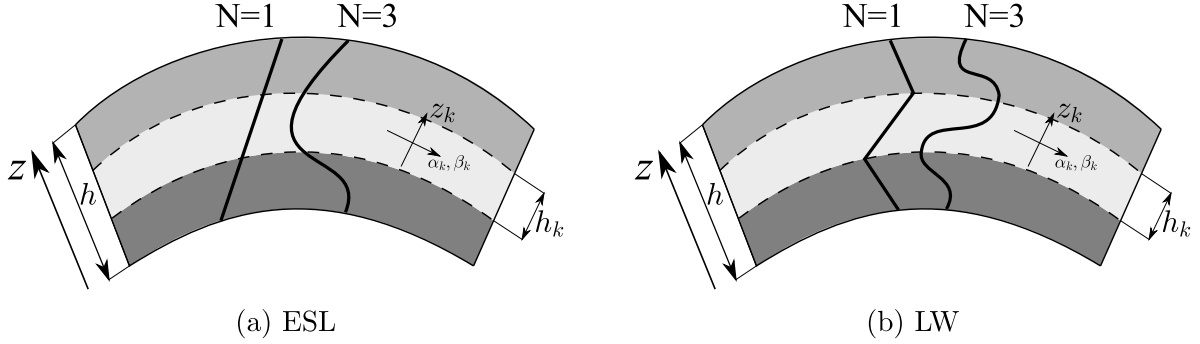

(a) ESL

(b) LW

Fig. 2. Behavior of the displacements along the thickness.

foundation for this approach is presented by Szabo and Babuška (1991). A key feature of HLE is its combination of a hierarchy in the structure of kinematic terms, akin to Taylor expansion, with a non-local distribution of mechanical unknowns across the thickness domain, similar to Lagrange expansion. These expansions are constructed based on the same cross-section discretization, and other functions, such as the hp-method for the CUF, are also adopted. For expressing the relationship involving one-dimensional Legendre polynomials, the most useful form is as follows:

$$L_p(\zeta) = \frac{2p+1}{p+1} L_{p-1}(\zeta) - \frac{p}{p+1} L_{p-2}(\zeta), \qquad p = 2, 3, \ldots \qquad (1)$$

where p represents the polynomial order. This relation is valid within the natural plane $\zeta = [-1, +1]$. The initial values for the Legendre polynomials are $L_0(\zeta) = 1$ and $L_1(\zeta) = \zeta$. A set of 1D functions can be defined out of this polynomials as:

$$F_1(\zeta) = \frac{1}{2} (1 - \zeta)$$
$$F_2(\zeta) = \frac{1}{2} (1 + \zeta) \qquad (2)$$
$$F_\tau(\zeta) = \phi_{\tau-1}(\zeta), \quad \tau = 3, 4, \ldots, p+1$$

with

$$\phi_j(r) = \sqrt{\frac{2j-1}{j}} \int_{-1}^{r} L_{j-1}(\zeta) d\zeta = \sqrt{\frac{1}{4j-1}} \left(L_j - L_{j-2} \right), \quad j = 2, 3, \ldots, p \qquad (3)$$

Fig. 1 shows an illustration of the plate section in the natural plane with $\zeta = [-1, +1]$.

3. Modeling approaches

In the development of theories for composite structures, two primary modeling techniques are commonly employed: the Equivalent-Single Layer (ESL) and the Layer Wise (LW) approaches. In this section, we provide a brief description of the behavior of displacements along the thickness of these composite structures.

In the ESL approach, the mathematical assumptions for the displacement field are consistent across all layers. For the sake of completeness, Fig. 2(a) illustrates the through-the-thickness distribution of displacements in this approach. Consequently, the resultant model considers variables for the entire composite structure and is independent of the number of layers. In this paper, Taylor polynomials are employed within ESL models. Furthermore, these polynomials can be enhanced by incorporating Zig-Zag functions, particularly the Murakami function. For more detailed information, please refer to Appendix B and the work of Carrera (2003). The inclusion of these functions allows for the satisfaction of the C_z^0-requirements (Carrera, 1996) for the displacement field along the thickness direction. In the domain of the structural theories, the displacements and the out-of-plane stresses must be piecewise continuous through the thickness, while their derivatives are discontinuous in the multilayered structures. In particular, according to the elasticity theory, the equilibrium and compatibility equations must be satisfied. If the ESL models are adopted, the derivatives of the displacements are continuous through the thickness, which does not permit to replicate the Zig-Zag behavior of the in-plane displacements. Then, the strains are continuous. When the strains are multiplied to the constitutive relations of each layer, the equilibrium equations are not satisfied. For this reason, even a higher order ESL theory is not sufficient to obtain good results, especially for the transverse stresses.

As far as LW approach concerns, different variables are described in each layer, independently from the other layers. Mechanical characteristics continuity is maintained at the interlaminar level, as depicted in Fig. 2(b). It is worth noting that the derivatives of the variables are not necessarily continuous at the interlaminar interfaces in this approach (i.e., C_z^0-requirements are naturally assured). The stress outcomes are comparable to exact and 3D solutions only if higher-order theories are adopted. In this paper, Legendre polynomials are employed within the LW models.

4. Node-dependent kinematics two-dimensional models

4.1. Preliminaries

Consider the shell depicted in Fig. 3. The shell mid-plane, denoted as Ω_0, lies in the (α, β) plane, while the section domain is defined along
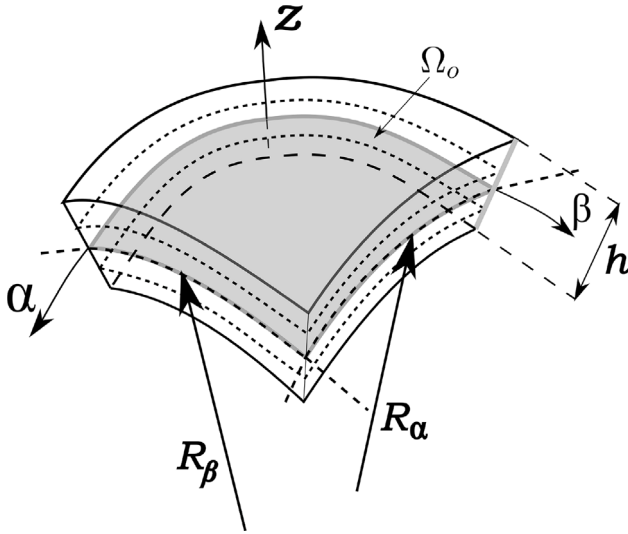
Fig. 3. Reference system for a multilayered shell.

the thickness direction z. The three-dimensional displacement vector for a multi-layered section shell in this reference system can be defined as follows:

$$\mathbf{u}^k(\alpha, \beta, z) = \left\{ u_\alpha^k(\alpha, z) \quad u_\beta^k(\alpha, \beta, z) \quad u_z^k(\alpha, \beta, z) \right\}^T \tag{4}$$

where k indicates the mathematical layer. The strain, ϵ^k, and stress, σ^k, components are herein arranged as:

$$\sigma^k = \left\{ \sigma_{\alpha\alpha}^k \quad \sigma_{\beta\beta}^k \quad \sigma_{zz}^k \quad \sigma_{\alpha z}^k \quad \sigma_{\beta z}^k \quad \sigma_{\alpha\beta}^k \right\}^T,$$
$$\epsilon^k = \left\{ \epsilon_{\alpha\alpha}^k \quad \epsilon_{\beta\beta}^k \quad \epsilon_{zz}^k \quad \epsilon_{\alpha z}^k \quad \epsilon_{\beta z}^k \quad \epsilon_{\alpha\beta}^k \right\}^T \tag{5}$$

where the strain vector are related to the displacements through the differential operator matrix $\mathbf{D}$ as

$$\epsilon^k = \mathbf{D}\mathbf{u}^k \tag{6}$$

The explicit form of the matrix of differential operators, $\mathbf{D}$, is defined in Appendix A.

The stress components can be determined using the constitutive equation as follows:

$$\sigma^k = \tilde{\mathbf{C}}^k \epsilon^k \tag{7}$$

where $\tilde{\mathbf{C}}^k$, is the matrix of the material coefficients, which is explicitly defined in Appendix A.

In the framework of 2D shell CUF, the 3D displacement field and its corresponding virtual variation can be conveniently expressed as follows:

$$\begin{array}{llll} \mathbf{u}^k(\alpha, \beta, z) & = & F_\tau(z)\mathbf{u}_\tau^k(\alpha, \beta), & \tau = 1, \dots, M \\ \delta\mathbf{u}^k(\alpha, \beta, z) & = & F_s(z)\delta\mathbf{u}_s^k(\alpha, \beta), & s = 1, \dots, M \end{array} \tag{8}$$

In this formulation, $F_\tau(z)$ represents the expansion functions along the thickness direction, and the Einstein convention is assumed for the repeated index τ. The parameter M represents the total number of expansions utilized. This formulation allows for the adoption of an infinite number of structural theories. For simplicity, Legendre-like and Taylor-like (with Zig-Zag functions using the Murakami function) functions are presented. In this paper, Taylor-like expansions (along with Zig-Zag functions) are employed in the *global* zone, as further detailed in Appendix B. For the shell formulation, Taylor expansion utilizes 1D polynomials z^i as a base, where i is a positive integer.

Subsequently, the displacement vector, denoted as $\mathbf{u}_\tau^k$, and the virtual variation, $\delta\mathbf{u}_s^k$, can be approximated using the Finite Element Method (FEM) as shown below:

$$\begin{array}{llll} \mathbf{u}_\tau^k(\alpha, \beta) & = & N_i(\alpha, \beta)\mathbf{u}_{\tau i}^k, & i = 1, \dots, N_n \\ \delta\mathbf{u}_s^k(\alpha, \beta) & = & N_j(\alpha, \beta)\delta\mathbf{u}_{sj}^k, & j = 1, \dots, N_n \end{array} \tag{9}$$

in which $N_i(\alpha, \beta)$ represents the shape functions, and N_n is the number of nodes within an element. The variable $\mathbf{u}_\tau^k(\alpha, \beta, z)$ signifies the nodal unknowns. For the numerical assessments in this work, the classical nine-node Lagrange (Q9) element is employed. Further information on this element can be found in Bathe (1996).

Consequently, by combining the CUF approximation (Eq. (8)) and the FEM discretization (Eq. (9)), the complete expression of FE displacement functions can be formulated:

$$\begin{array}{llll} \mathbf{u}^k(\alpha, \beta, z) & = & N_i(\alpha, \beta)F_\tau(z)\mathbf{u}_{\tau i}^k, & \tau = 1, \dots, M; \quad i = 1, \dots, N_n \\ \delta\mathbf{u}^k(\alpha, \beta, z) & = & N_j(\alpha, \beta)F_s(z)\delta\mathbf{u}_{sj}^k, & s = 1, \dots, M; \quad j = 1, \dots, N_n \end{array} \tag{10}$$

4.2. Node-dependent kinematics

An additional advancement can be achieved by anchoring the thickness functions with the nodes of shell finite elements. Essentially, every FE node possesses its unique set of structural theories. This concept can be expressed mathematically as follows:

$$\begin{array}{llll} \mathbf{u}^k(\alpha, \beta, z) & = & N_i(\alpha, \beta)F_\tau^i(z)\mathbf{u}_{\tau i}^k, & \tau = 1, \dots, M_i; \quad i = 1, \dots, N_n \\ \delta\mathbf{u}^k(\alpha, \beta, z) & = & N_j(\alpha, \beta)F_s^j(z)\delta\mathbf{u}_{sj}^k, & s = 1, \dots, M_j; \quad j = 1, \dots, N_n \end{array} \tag{11}$$

Eq. (11) defines a family of two-dimensional FE models with NDK. This type of element allows for the straightforward adoption of different kinematic theories within the same element. This approach facilitates local kinematic refinement on the nodal level. For the sake of clarity, Fig. 4 illustrates a four-node element (Q4) in which various theories are employed. Taylor-like (including Zig-Zag functions) and Legendre-like expansions can be applied without the need for additional mathematical complexities. In particular, HLE2 has three expansions for each layer, TEZ2 is associated to four expansions, while TE2 has three expansions. For example, the in-plane displacement u_α^k for this element can be expressed as shown below:

$$u_\alpha^k(\alpha, \beta, z) = N_1 \overbrace{\left(F_1^1 u_{\alpha_{11}}^k + F_2^1 u_{\alpha_{21}}^k + F_3^1 u_{\alpha_{31}}^k \right)}^{\text{HLE2}}$$

$$+ N_2 \overbrace{\left(F_1^2 u_{\alpha_{12}} + F_2^2 u_{\alpha_{22}} + F_3^2 u_{\alpha_{32}} + F_4^2 u_{\alpha_{42}} \right)}^{\text{TEZ2}}$$

$$+ N_3 \underbrace{\left(F_1^3 u_{\alpha_{13}} + F_2^3 u_{\alpha_{23}} + F_3^3 u_{\alpha_{33}} \right)}_{\text{TE2}} + N_4 \underbrace{\left(F_1^4 u_{\alpha_{14}} + F_2^4 u_{\alpha_{24}} + F_3^4 u_{\alpha_{34}} \right)}_{\text{TE2}} \tag{12}$$

The following explains the meaning of the expansion functions for each FE node:

- F_1^1 and F_2^1 : linear terms of Legendre expansion, see Eq. (2);
- F_3^1: parabolic term of Legendre expansion, see Eq. (2);
- $F_1^2 = F_1^3 = F_1^4$: constant terms of Taylor expansion, see Eqs. (25) and (27);
- $F_2^2 = F_2^3 = F_2^4$: linear terms of Taylor expansion, see Eqs. (25) and (27);
- $F_3^2 = F_3^3 = F_3^4$: parabolic terms of Taylor expansion, see Eqs. (25) and (27);
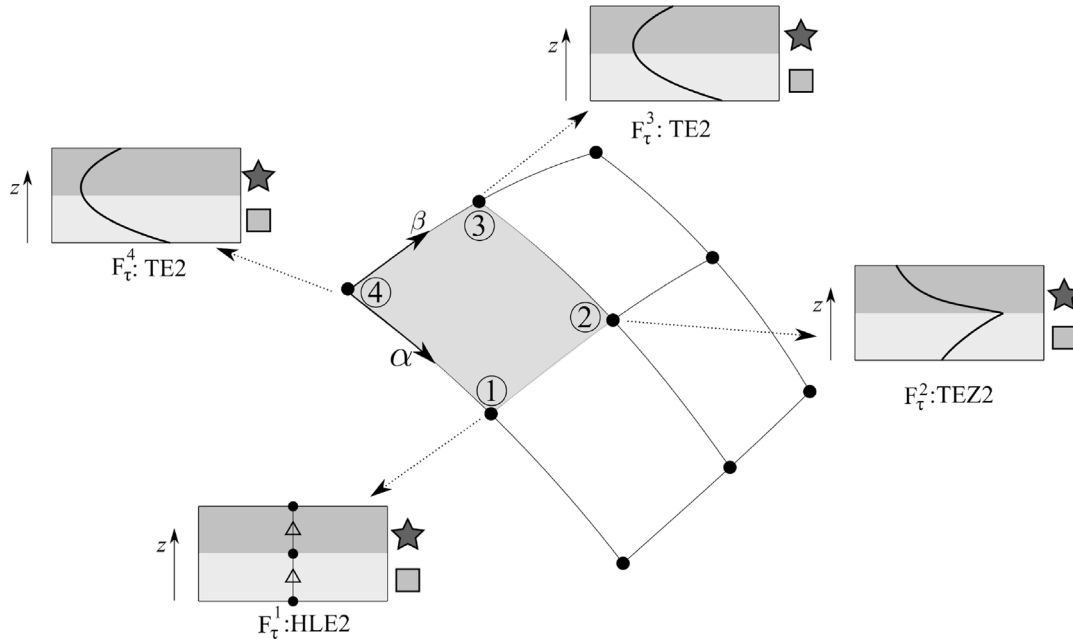- F_4^2 : Murakami Zig-Zag function, see Eq. (27).

Fig. 4. A four-node shell element with node-dependent kinematics.

4.3. FE governing equations

The principle of virtual displacements is used to derive the governing equations:

$$\delta L_{int} = \delta L_{ext} \tag{13}$$

In the provided equation, δL_{int} signifies the virtual variation of the internal work, whereas δL_{ext} denotes the virtual variation of the external work. The expression for δL_{int} can be written as:

$$\delta L_{int} = \int_{V_k} \delta \boldsymbol{\epsilon}^T \boldsymbol{\sigma} H_\alpha H_\beta \mathrm{d}\alpha \mathrm{d}\beta \mathrm{d}z \tag{14}$$

See Appendix A for the definition of H_α and H_β. By using the CUF-type displacement functions (Eq. (11)), the geometric relations in Eq. (6), and constitutive equations (Eq. (7)), the following expression can be obtained:

$$\delta L_{int} = \delta \mathbf{u}_{sj}^{kT} \int_{V_k} \left(\mathbf{D} F_s^j N_j\right)^T \tilde{\mathbf{C}}^k \left(\mathbf{D} F_\tau^i N_i\right) H_\alpha H_\beta \mathrm{d}\alpha \mathrm{d}\beta \mathrm{d}z \, \mathbf{u}_{\tau i}^k = \delta \mathbf{u}_{sj}^{kT} \mathbf{K}_{ij\tau s}^k \mathbf{u}_{\tau i}^k \tag{15}$$

where $\mathbf{K}_{ij\tau s}^k$ is the fundamental nucleus (FN) of the stiffness matrix for NDK FE models. The explicit expression of $\mathbf{K}_{ij\tau s}^k$ is provided as follows:

$$\mathbf{K}_{ij\tau s}^k = \int_{V_k} \left(\mathbf{D} F_s^j N_j\right)^T \tilde{\mathbf{C}}^k \left(\mathbf{D} F_\tau^i N_i\right) H_\alpha H_\beta \mathrm{d}\alpha \mathrm{d}\beta \mathrm{d}z \tag{16}$$

The virtual work δL_{ext} done by the external load $\mathbf{p}$ is expressed as follows:

$$\delta L_{ext} = \int_{V_k} \delta \mathbf{u}^{kT} \mathbf{p}^k H_\alpha H_\beta \mathrm{d}\alpha \mathrm{d}\beta \mathrm{d}z \tag{17}$$

The above equation can be further written in the form of CUF as:

$$\delta L_{ext} = \delta \mathbf{u}_{sj}^{kT} \int_{V_k} N_j F_s^j \mathbf{p}^k H_\alpha H_\beta \mathrm{d}\alpha \mathrm{d}\beta \mathrm{d}z = \delta \mathbf{u}_{sj}^{kT} \mathbf{P}_{sj}^k \tag{18}$$

where $\mathbf{P}_{sj}^k$ represents the FN of the load vector. Hence, the governing equation for the shell FE models with NDK is described by the following relation:

$$\mathbf{K}_{ij\tau s}^k \mathbf{u}_{\tau i}^k = \mathbf{P}_{sj}^k \tag{19}$$

In the present work, the Mixed Interpolation of Tensorial Component (MITC) method is adopted to counteract the shear locking issues. For the sake of brevity, the extended formulation is not shown. More information can be found in Cinefra and Valvano (2016).

4.4. Assembly of the stiffness matrix

In the preceding section, the fundamental nucleus was described as the 3×3 core unit of the stiffness matrix. Conversely, the FN of the load vector is 3×1. By iterating through the superscripts, the stiffness matrix can be determined on both the node and element levels, and subsequently assembled at the structural level. For more in-depth information, please refer to Carrera et al. (2014).

Fig. 5 illustrates a portion of the assembly process for the stiffness matrix and load vector in models featuring node-dependent kinematics. This matrix is based on the example presented in Fig. 4. When different models are utilized within a single element, K^{ij} becomes rectangular instead of square if $M_i \neq M_j$. For example, if the number of expansion terms at node 1 is $M_1 = 5$, while at the fourth node it is $M_4 = 3$, the dimensions of the matrices are as follows: $\mathbf{K}^{11}$ is a 15×15 matrix, $\mathbf{K}^{44}$ is a 9×9 matrix, $\mathbf{K}^{14}$ is a 15×9 matrix, and $\mathbf{K}^{41}$ is a 9×15 matrix. The load vector must be constructed accordingly to match the stiffness matrix.

5. Numerical results

In this section, the displacement and stress fields are analyzed for two benchmark cases. These results are then compared with reference solutions from the open literature. The first benchmark involves an homogeneous simply-supported cylindrical shell subjected to two pinching loads. The second benchmark features a three-layer spherical shell loaded by a bisinusoidal local pressure.

Different variable kinematic models have been considered and compared. The models have been named as follows:

- HLEm indicates Hierarchical Legendre Expansion;
- TEm stands for Taylor Expansion;
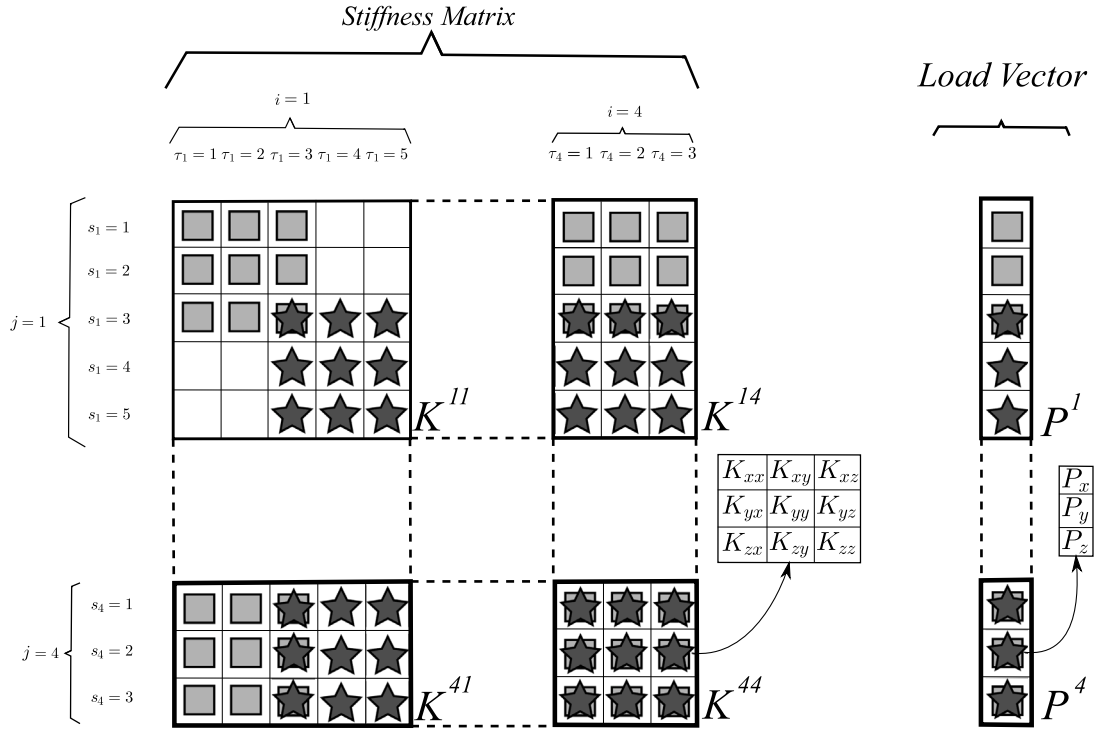- TEZm represents Taylor Expansion with the Murakami Zig-Zag function (MZZF).

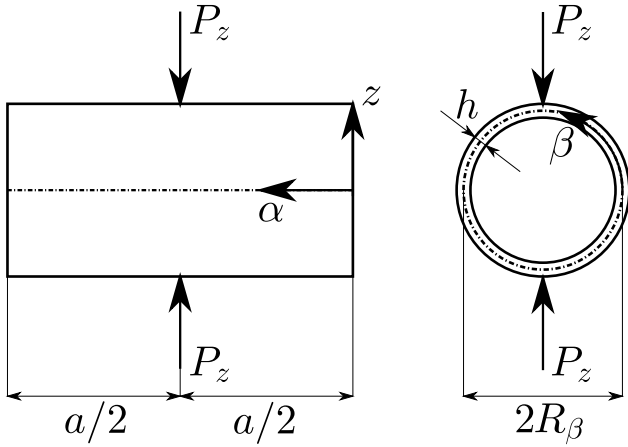**Fig. 5.** Assembly of the stiffness matrix and load vector of models with node-dependent kinematics.

Fig. 6. Geometrical properties and loading conditions of the homogeneous cylindrical shell under two pinching loads.
Source: The study case is taken from Lindberg et al. (1969).

Fig. 7. Homogeneous cylindrical shell under two pinching loads. Scheme of the NDK method. Adoption of a 13 × 13 FEM discretization.

Here, m corresponds the polynomial order. For the sake of clarity, the notation of the NDK models is detailed later for each study case.

For both study cases, the refined theories are used in the area around the localized load.

5.1. Homogeneous cylindrical shell under two pinching loads

The first considered benchmark is a cylindrical shell. Lindberg et al. (1969) first proposed the analysis. Fig. 6 shows the geometrical properties of the structure. The geometrical data are $a/R_\beta = 2$, $R_\beta/h = 100$, and $b = 2\pi R_\beta$. An isotropic material is considered and its properties are: E = 3×10^6 [psi] and $v = 0.3$. The cylinder is simply supported at $\alpha = 0$ and $\alpha = a$. Two concentrated forces, P_z, are applied. See Fig. 6. These loads are posed in $[a/2, b/4, h/2]$ and are equal to 10^4 [lb]. A comparison with Flügge equations (Flügge, 1934) calculated by
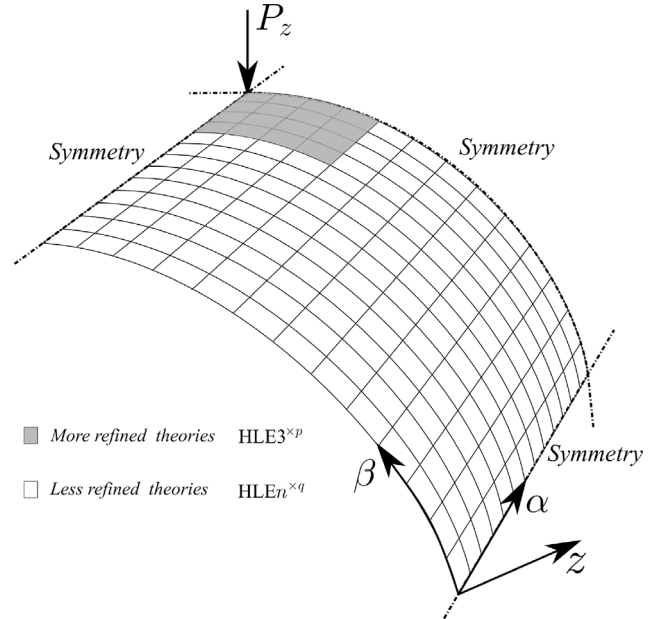
Lindberg et al. (1969) is given. In this study case, transverse displacements, u_z, are studied. The dimensionless displacements are given as follows:
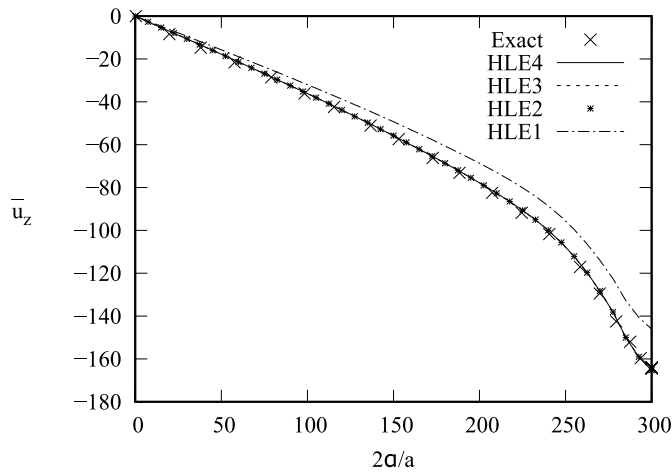
$$\bar{u}_z = \frac{Eh}{P_z} u_z \qquad (20)$$

Taking advantage of the symmetry feature of the structure and loading conditions, an octave of the cylinder is discretized with finite elements. Symmetric boundary conditions are imposed, as illustrated in Fig. 7. A uniform mesh grid of 13 × 13 elements is employed for all the analyses

Table 1
Transverse displacements evaluated in $[a/2, b/4, 0]$ for the homogeneous cylindrical shell under two pinching loads.

Model	$\bar{u}_z$	DOF
Literature		
Exact (Lindberg et al., 1969)	−164.24	–
Present-uniform models		
HLE4	−165.42	10 935
HLE3	−165.42	8748
HLE2	−165.23	6561
HLE1	−146.04	4374
Present-NDK models		
HLE3$^{×4}$-HLE2$^{×165}$	−165.39	6636
HLE3$^{×4}$-HLE1$^{×165}$	−158.60	4524
HLE3$^{×16}$-HLE2$^{×153}$	−165.41	6804
HLE3$^{×16}$-HLE1$^{×153}$	−162.44	4860
HLE3$^{×36}$-HLE2$^{×133}$	−165.41	7062
HLE3$^{×36}$-HLE1$^{×133}$	−164.01	5372

Fig. 8. Homogeneous cylindrical shell under two pinching loads. Transverse displacements evaluated along the line $[\alpha, b/4, 0]$ for the uniform models Exact solution from Lindberg et al. (1969).

in this study. While the convergence analysis has been conducted, it is not presented here for the sake of conciseness.

Several structural theories are used. First, uniform Legendre HLE1, HLE2, HLE3, and HLE4 models are adopted for comparison purposes. Then, NDK models are considered. In particular, Fig. 7 shows a simplified scheme of the NDK method. HLE3 kinematics is adopted as a local refinement around the loaded zone. Less refined theories are used in the remainder of the shell, namely HLE1 and HLE2. FE models with node-dependent kinematics are denoted by HLE$m^{×p}$-HLE$n^{×q}$. In particular, the upper scripts denote the number of elements of the shell elements adopting the corresponding kinematics. Three different configurations of NDK models are used: HLE3$^{×4}$-HLE$n^{×165}$, HLE3$^{×4}$-HLE$n^{×153}$ (illustrated in Fig. 7), and HLE3$^{×36}$-HLE$n^{×133}$.

Table 1 compares the results of the present uniform and NDK models, with the reference solution. This is useful to understand the differences between the lower-order theories, while using the same DOF. Displacement results are given in the central column, while the DOFs are reported in the third column. Fig. 8 depicts the transverse displacements along the line $[\alpha, b/4, 0]$. In this figure, the reference solution and the results from the uniform models are compared. Fig. 9 illustrates the trends for the NDK models. Specifically, Figs. 9(a) and 9(b) present the results for the NDK models using HLE1 and HLE2 in the global part of the structure, respectively.

Here are some important remarks based on the results:

1. The results show excellent agreement with the reference solution;
2. This analysis highlights the necessity of employing refined models, such as HLE3, to accurately investigate displacement behavior in the vicinity of a point force;
3. Remarkably accurate results are achieved when combining HLE3 and HLE2;
4. Enhancing the area where a local model is employed significantly improves the accuracy of the solution, especially when HLE1 is used in the global region.

5.2. Three layer shell loaded by bisinusoidal localized pressure

The second case study involves the analysis of a three-layered cross-ply spherical shell. The three layers have an equal thickness of $h/3$. The shell is loaded with a local bi-sinusoidally distributed pressure applied at the center of the shell's top layer, as depicted in Fig. 10. The origin point of the curvilinear reference system is positioned at the central point of the spherical shell. The middle-surface radii are assumed to be $R_\alpha = R_\beta = R = 1$. A radius-to-thickness ratio of $R/h = 10$ is considered. The local pressure is applied to the top surface, and its distribution follows:

$$p(\alpha, \beta) = -p_0 \cos \frac{\pi\alpha}{a/10} \cos \frac{\pi\beta}{b/5} \tag{21}$$

where a and b represent the dimensions of the spherical shells in α and β direction, respectively, while $p_0 = 1$ [Pa] is the magnitude of the pressure load. The loaded region covers the central area of $\frac{a}{10} \times \frac{b}{5}$. The laminae have the following material properties: $E_L = 25 E_T$, $E_T = E_z$, $G_{Lz} = G_{LT} = 0.5 E_T$, $G_{Tz} = 0.5 E_T$, and $\nu_{LT} = \nu_{Lz} = \nu_{Tz} = 0.25$. L stands for the longitudinal direction, and T for the transverse one. z indicates the thickness coordinate. The lamination sequence is $[90/0/90]°$. The shell is simply supported with correspondence to its four edges. For comparison purposes, the transverse displacements and the stresses are expressed in the following dimensionless parameters:

$$\bar{w} = -\frac{10^6 E_L h^3}{p_0 R^4} w, \quad \bar{\sigma}_{\beta\beta} = -\frac{10^4 h^2}{p_0 R^2} \sigma_{\beta\beta},$$

$$\bar{\sigma}_{\beta z} = \frac{10^2 h}{p_0 R} \sigma_{\beta z}, \quad \bar{\sigma}_{zz} = -\frac{1}{p_0} \sigma_{zz} \tag{22}$$

Utilizing the structural and loading symmetry of the configuration, a quarter of the shell is modeled with finite elements, employing symmetric boundary conditions, as shown in Fig. 11. This case corresponds to the one presented by Li et al. (2019), where results were provided through a finite element analysis conducted using the commercial software ABAQUS. In particular, C3D20R (20-node quadratic brick element with reduced integration) is used to build 3D FE models.

A uniform mesh grid of 20×20 elements is utilized for all the analyses in this benchmark. For the sake of brevity, the convergence analysis is not presented. Various structural theories are employed. Initially, uniform Legendre HLE1, HLE2, and HLE5 models, Taylor TE3 and TE6, and Taylor models with Murakami functions TEZ2 and TEZ5 are used for comparative purposes. Subsequently, NDK models are introduced. In particular, Fig. 11 illustrates a simplified scheme of the NDK method. A local refinement is applied around the loaded zone, where a HLE5 model is adopted, while less refined theories are employed for the remaining part of the shell. In contrast to the previous example, the superscripts in the notation are omitted here. The same configuration is used for all the NDK models, where 24 elements adopt HLE5, while 376 elements implement lower-order theories.

Transverse displacements, w, in-plane stresses, $\sigma_{\beta\beta}$, shear stresses, $\sigma_{\beta z}$, and transverse stresses, σ_{zz}, are assessed in the vicinity of the applied pressure. Six different combinations of NDK models are employed: HLE5-HLE2, HLE4-TEZ5, HLE5-TE6, HLE5-HLE1, HLE5-TEZ2, and HLE4-TE3. The first three NDK theories have 35 301 degrees of freedom, while the latter three have 20 172 degrees of freedom.
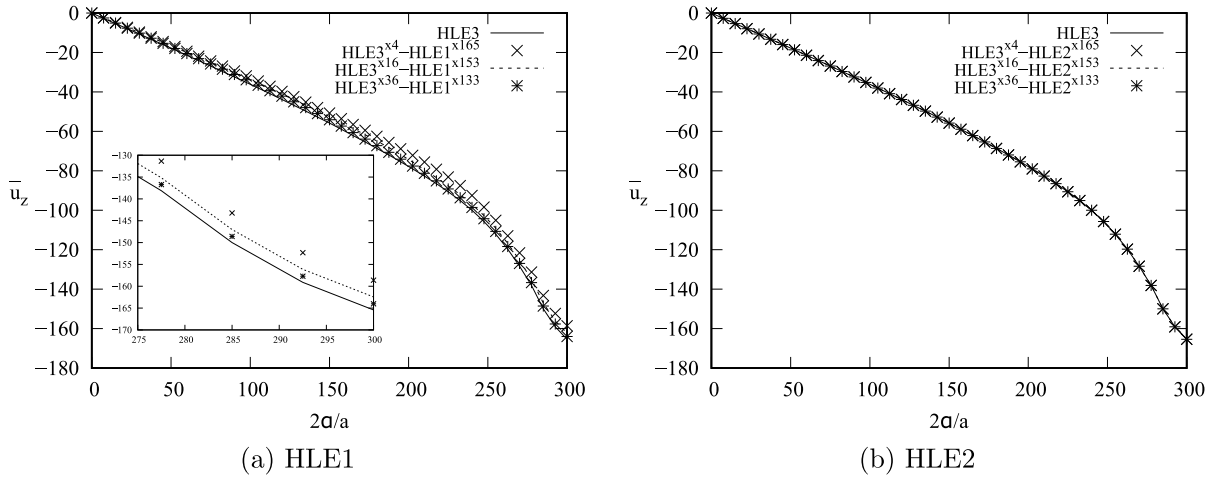
(a) HLE1
(b) HLE2

Fig. 9. Homogeneous cylindrical shell under two pinching loads. Transverse displacements evaluated along the line $[\alpha, b/4, 0]$ for the NDK models.
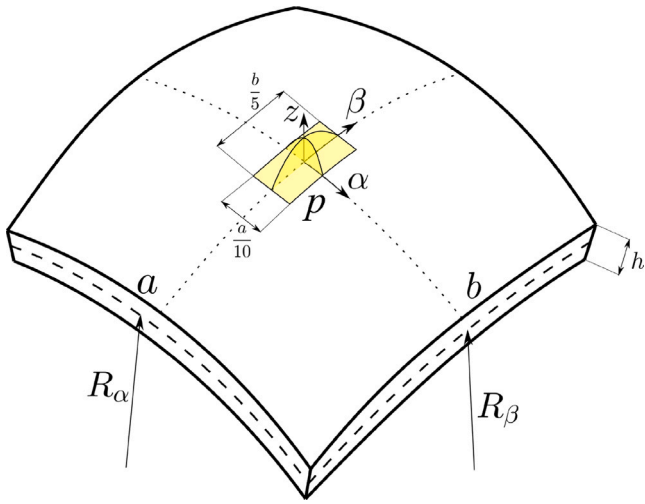

Fig. 10. Geometrical properties and loading conditions of the three layer shell loaded by bisinusoidal localized pressure.
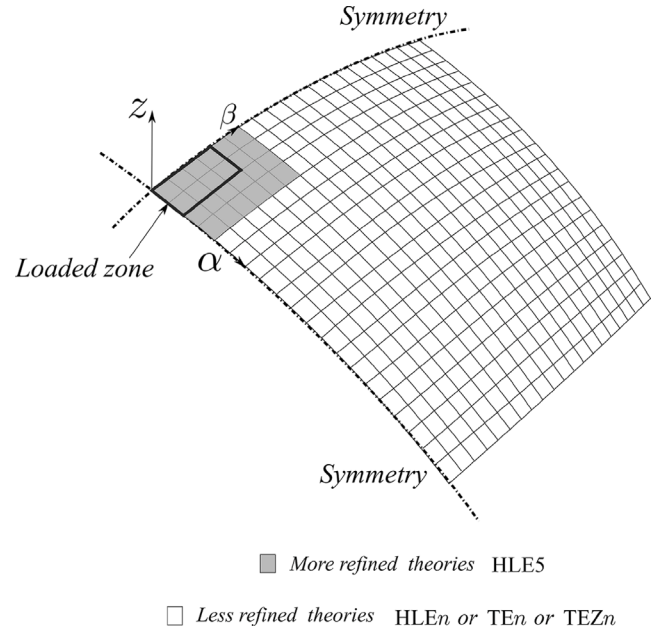*Source:* The study case is taken from Li et al. (2019).

Table 2 compared the results obtained from the models considered in this study with those from the literature. The reference solution, uniform solutions, and NDK solutions are compared. This comparison helps in understanding the differences between the lower-order theories while maintaining the same number of degrees of freedom (DOF). Displacements and stresses are provided in the central columns, and the DOFs are reported in the last column for the purpose of comparison. In all the figures presented, the left graph compares uniform models with reference solutions, while the right diagram compares the HLE5 solution with the NDK models. Figs. 12(a) and 12(b) illustrate the trend of shear stress along the thickness for higher-order models, while Figs. 13(a) and 13(b) show the results when HLE1, TEZ2, and TE3 are used as global theories.

The analysis yields the following results:

1. Refined models are essential in the vicinity of the loaded zone for accurate results;
2. It is worth to remark that even an higher-order ESL, i.e. TE6, is not sufficient to obtain acceptable results for the shear stresses;
3. The NDK method offers a way to combine the accuracy of LW models and the computational efficiency of ESL models,

Fig. 11. Three layer shell loaded by bisinusoidal localized pressure. Scheme of the NDK method. Adoption of a 20×20 FEM discretization.

resulting in optimal shells models, particularly for models using the Murakami Zig-Zag function (TEZ);
4. Implementing HLE-HLE models, which means using LW-LW models, significantly accelerates the analysis while keeping the DOFs low;
5. Figs. 12(b) and 13(b) clearly demonstrates how the shear stresses can be accurately described. At the same time, the NDK methods permit to diminish the computational cost, since the refined theories are used in a small portion of the computational domain. The proposed models are particularly cost-efficient if lower-order expansions are used in the 'global' zone.

6. Conclusions

In this paper, a class of refined 2D shell FE models with node-dependent kinematics is presented for the global–local analysis of homogeneous and composite curved structures. The present shell formulation is able to accurately account for different type of structures
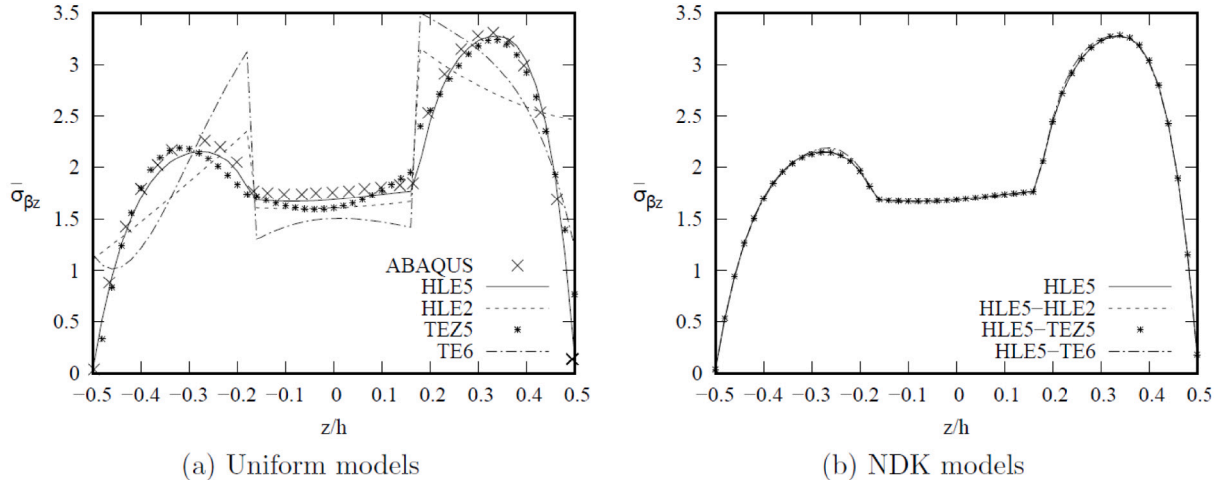
Fig. 12. Three layer shell loaded by bisinusoidal localized pressure. Shear stresses evaluated in $[0, 2b/25, z]$ for HLE2, TEZ5, and TE6. ABAQUS solution from Li et al. (2019).
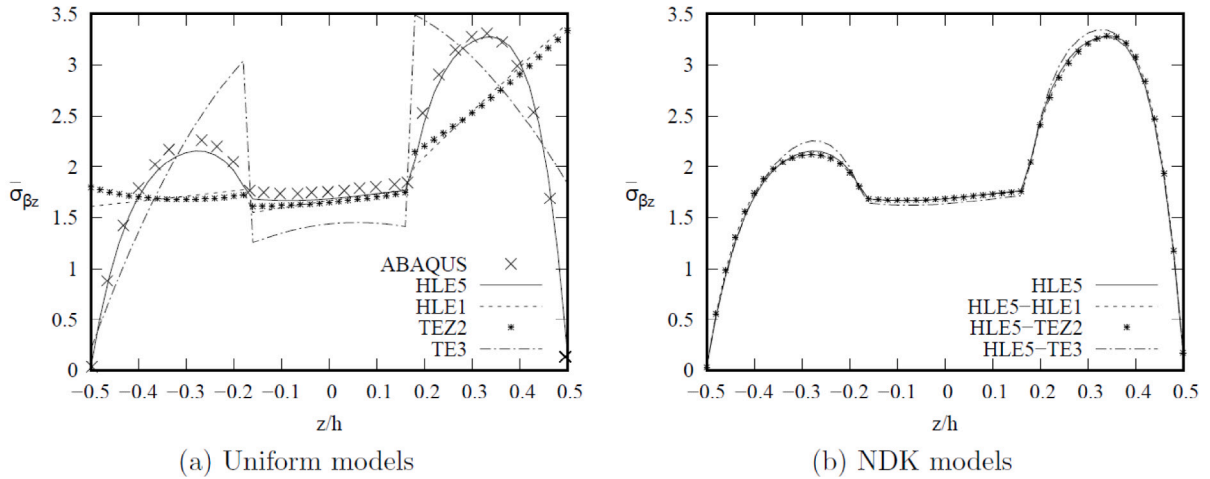

Fig. 13. Three layer shell loaded by bisinusoidal localized pressure. Shear stresses evaluated in $[0, 2b/25, z]$ for HLE1, TEZ2, and TE3. ABAQUS solution from Li et al. (2019).

Table 2
Transverse displacement and stresses for a three layer shell loaded by bisinusoidal localized pressure.

Model	$\overline{w}$ $[0, 0, 0]$	$\overline{\sigma}_{\beta\beta}$ $[0, 0, h/2]$	$\overline{\sigma}_{\beta z}$ $[0, 2b/25, 0]$	$\overline{\sigma}_{zz}$ $[0, 0, h/2]$	DOF
Literature-ABAQUS					
C3D20R (Li et al., 2019)	5680	528.2	1.757	1.001	950 283
Present-uniform models					
HLE5	5727	538.4	1.687	1.005	80 688
HLE2	5677	497.1	1.605	1.006	35 301
HLE1	5607	415.2	1.666	0.8625	20 172
TEZ5	5711	532.1	1.606	1.017	35 301
TEZ2	5596	429.2	1.649	0.9964	20 172
TE6	5614	527.8	1.504	1.011	35 301
TE3	5571	496.2	1.439	1.104	20 172
Present-NDK models					
HLE5-HLE2	5716	538.1	1.686	1.005	38 460
HLE5-HLE1	5672	537.8	1.689	1.005	24 384
HLE5-TEZ5	5720	538.9	1.686	1.005	38 460
HLE5-TEZ2	5672	537.8	1.687	1.005	24 384
HLE5-TE6	5670	539.4	1.673	1.005	38 460
HLE5-TE3	5620	537.3	1.634	1.005	24 384

and curvatures. This ability is crucial when shallow structures are considered. Hierarchical Legendre Expansions (HLE) are adopted as through-the-thickness functions for the local refinement on the nodal level. In particular, the present advancements enable the use of HLE with various polynomial orders within the same model. Additionally, Taylor expansions, including the incorporation of the Murakami Zig-Zag function, can be applied in the global zone. To demonstrate the capabilities of this approach, two well-established case studies, homogeneous cylindrical and composite spherical shells, are selected from the open literature. A comprehensive analysis is conducted, considering various boundary and load conditions, as well as different material properties.

The outcomes obtained through the developed NDK FEs are meticulously compared with analytical and numerical solutions whenever feasible. The following concluding remarks can be made:

1. By combining HLE with NDK method, computational efficiency is enhanced for the analysis of both homogeneous and three-layer shells;
2. This approach allows the incorporation of two or more different kinematics (i.e. theories of structures) in the same model, enabling the use of various types of polynomials and polynomial orders;
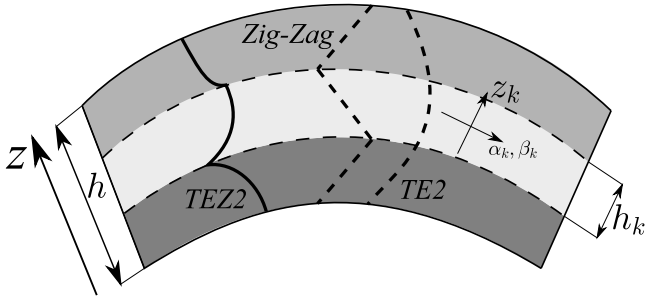
Fig. 14. Geometrical meaning of Murakami's Zig-Zag function.

3. Local kinematic refinement can be implemented without the need to alter the finite element mesh, providing flexibility in modeling;
4. Models using HLE-HLE and HLE-TEZ combinations can accurately predict displacement and stress results;
5. Within the Carrera Unified Formulation (CUF), the structural finite element formulations are compact and do not require additional coupling or superposition.

However, some drawbacks are present in the NDK method. First, more degrees of freedom are used if compared to the monolithic low-order models. Second, the individuation of the 'local' zone, which can be rather cumbersome, and it is problem dependent. In the considered examples, it was easy to identify the most critical zone. In other cases, the 'local' zone and the loaded one could not be coincident. See Zappino et al. (2023) for more details. It is shown that the refined zone could be in several portions of the structures, depending on what the researcher wants to evaluate.

CRediT authorship contribution statement

E. Carrera: Conceptualization, Funding acquisition, Methodology, Project administration, Resources, Supervision, Writing – review & editing. **A. Pagani:** Investigation, Methodology, Supervision, Writing – review & editing. **D. Scano:** Formal analysis, Investigation, Software, Validation, Visualization, Writing – original draft.

Declaration of competing interest

The authors declare that they have no known competing financial interests or personal relationships that could have appeared to influence the work reported in this paper.

Data availability

Data will be made available on request.

Appendix A. Matrix of differential operators and matrix of material coefficients

For problems with infinitesimal strains, the explicit form of the matrix of differential operators, **D**, can be written as follows:

$$\mathbf{D} = \begin{bmatrix} \frac{\partial_\alpha}{H_\alpha} & 0 & \frac{1}{H_\alpha R_\alpha} \\ 0 & \frac{\partial_\beta}{H_\beta} & \frac{1}{H_\beta R_\beta} \\ 0 & 0 & \partial_z \\ \partial_z - \frac{1}{H_\alpha R_\alpha} & 0 & \frac{\partial_\alpha}{H_\alpha} \\ 0 & \partial_z - \frac{1}{H_\beta R_\beta} & \frac{\partial_\beta}{H_\beta} \\ \frac{\partial_\beta}{H_\beta} & \frac{\partial_\alpha}{H_\alpha} & 0 \end{bmatrix} \tag{23}$$

where $\partial_\alpha = \frac{\partial(\cdot)}{\partial \alpha}$, $\partial_\beta = \frac{\partial(\cdot)}{\partial \beta}$, $\partial_z = \frac{\partial(\cdot)}{\partial z}$, $H_\alpha = 1 + \frac{z}{R_\alpha}$, and $H_\beta = 1 + \frac{z}{R_\beta}$. It is possible to return to the plate formulation if R_α and R_β tend to infinity. Thus, H_α and H_β can considered equal to one, and the matrix is thus simplified.

The explicit expression of the matrix of material coefficients is defined as follows:

$$\mathbf{C} = \begin{bmatrix} C_{11} & C_{12} & C_{13} & 0 & 0 & C_{16} \\ C_{12} & C_{22} & C_{23} & 0 & 0 & C_{26} \\ C_{13} & C_{32} & C_{33} & 0 & 0 & C_{36} \\ 0 & 0 & 0 & C_{44} & C_{45} & 0 \\ 0 & 0 & 0 & C_{45} & C_{55} & 0 \\ C_{16} & C_{26} & C_{36} & 0 & 0 & C_{66} \end{bmatrix} \tag{24}$$

Appendix B. Taylor polynomials and the Murakami zig-zag function

In this paper, Taylor-based polynomials and Zig-Zag Taylor-based polynomials are employed as expansion functions for evaluating displacements across the thickness of composite structures. In the shell formulation, 1D polynomials z^i are used (where i is a positive integer) to construct the Taylor-like expansions:

$$\mathbf{u} = F_1 \mathbf{u}_1 + F_2 \mathbf{u}_2 + \cdots + F_M \mathbf{u}_M = F_\tau \mathbf{u}_\tau, \qquad \tau = 1, \ldots, M \tag{25}$$

$$F_1 = z^0 = 1, \quad F_2 = z^1 = 1, \quad \cdots, \quad F_M = z^{M-1}, \tag{26}$$

While Taylor-based models are unable to capture the Zig-Zag effect, the discontinuity of the first derivative at the layer interfaces in the ESL approach can be addressed by utilizing the MZZF. To facilitate this, an adimensional layer coordinate $\zeta_k = z_k/2h_k$ is introduced, where h_k represents the thickness of the kth layer, and z_k is the layer thickness coordinate. An example of a Taylor second-order expansion enhanced with the MZZF is provided below:

$$u_\alpha(\alpha, \beta, z) = u_{\alpha_1} + z u_{\alpha_2} + z^2 u_{\alpha_3} + (-1)^k \zeta_k u_{\alpha_4}$$
$$u_\beta(\alpha, \beta, z) = u_{\beta_1} + z u_{\beta_2} + z^2 u_{\beta_3} + (-1)^k \zeta_k u_{\beta_4} \tag{27}$$
$$u_z(\alpha, \beta, z) = u_{z_1} + z u_{z_2} + z^2 u_{z_3} + (-1)^k \zeta_k u_{z_4}$$

For the sake of clarity, Fig. 14 illustrates the Murakami function, the second-order Taylor expansion, and their sum, which results in an enhanced second model.

References

Airoldi, A., Baldi, A., Bettini, P., Sala, G., 2015. Efficient modelling of forces and local strain evolution during delamination of composite laminates. Composites B 72, 137–149.

Aitharaju, V.R., 1999. C° zigzag kinematic displacement models for the analysis of laminated composites. Mech. Compos. Mater. Struct. 6 (1), 31–56.

Aminpour, M.A., Ransom, J.B., McCleary, S.L., 1995. A coupled analysis method for structures with independently modelled finite element subdomains. Internat. J. Numer. Methods Engrg. 38 (21), 3695–3718.

Argyris, J.H., 1966. Matrix displacement analysis of plates and shells. Ing. Arch. 35, 102–142.

Bathe, K.J., 1996. Finite Element Procedure. Prentice hall, Upper Saddle River, New Jersey, USA.

Bathe, K.-J., Dvorkin, E.N., 1986. A formulation of general shell elements—the use of mixed interpolation of tensorial components. Internat. J. Numer. Methods Engrg. 22, 697–722.

Biscani, F., Giunta, G., Belouettar, S., Carrera, E., Hu, H., 2012. Variable kinematic plate elements coupled via arlequin method. Internat. J. Numer. Methods Engrg. 91 (12), 1264–1290.

Blanco, P.J., Feijóo, R.A., Urquiza, S.A., 2008. A variational approach for coupling kinematically incompatible structural models. Comput. Methods Appl. Mech. Engrg. 197 (17), 1577–1602.

Blanco, P., Gervasio, P., Quarteroni, A., 2011. Extended variational formulation for heterogeneous partial differential equations. Comput. Methods Appl. Math. 11 (2), 141–172.

Bucalém, M.L., Bathe, K.J., 1993. Higher-order MITC general shell elements. Internat. J. Numer. Methods Engrg. 36, 3729–3754.

Carrera, E., 1996. C° Reissner–Mindlin multilayered plate elements including zig-zag and interlaminar stress continuity. Internat. J. Numer. Methods Engrg. 39 (11), 1797–1820.

Carrera, E., 1998. Evaluation of layerwise mixed theories for laminated plates analysis. AIAA J. 36 (5), 830–839.

Carrera, E., 2001. Developments, ideas, and evaluations based upon Reissner's mixed variational theorem in the modeling of multilayered plates and shells. Appl. Mech. Rev. 54 (4), 301–329.

Carrera, E., 2003. Historical review of zig-zag theories for multilayered plates and shells. Appl. Mech. Rev. 56 (3), 287–308.

Carrera, E., Cinefra, M., Petrolo, M., Zappino, E., 2014. Finite Element Analysis of Structures Through Unified Formulation. John Wiley & Sons.

Carrera, E., Demasi, L., 2002. Classical and advanced multilayered plate elements based upon PVD and RMVT. Part 1: Derivation of finite element matrices. Internat. J. Numer. Methods Engrg. 55 (2), 191–231.

Carrera, E., Pagani, A., Petrolo, M., 2013. Use of Lagrange multipliers to combine 1D variable kinematic finite elements. Comput. Struct. 129, 194–206.

Carrera, E., Pagani, A., Valvano, S., 2017. Multilayered plate elements accounting for refined theories and node-dependent kinematics. Composites B 114, 189–210.

Carrera, E., Valvano, S., Kulikov, M., 2018. Electro-mechanical analysis of composite and sandwich multilayered structures by shell elements with node-dependent kinematics. Int. J. Smart Nano Mater. 9 (1), 1–33.

Carrera, E., Zappino, E., 2017. One-dimensional finite element formulation with node-dependent kinematics. Comput. Struct. 192, 114–125.

Cho, Y.B., Averill, R.C., 2000. First-order zig-zag sublaminate plate theory and finite element model for laminated composite and sandwich panels. Compos. Struct. 50 (1), 1–15.

Cho, M., Oh, J., 2004. Higher order zig-zag theory for fully coupled thermo-electric–mechanical smart composite plates. Int. J. Solids Struct. 41 (5), 1331–1356.

Cinefra, M., Carrera, E., 2013. Shell finite elements with different through-the-thickness kinematics for the linear analysis of cylindrical multilayered structures. Internat. J. Numer. Methods Engrg. 93 (2), 160–182.

Cinefra, M., Valvano, S., 2016. A variable kinematic doubly-curved MITC9 shell element for the analysis of laminated composites. Mech. Adv. Mater. Struct. 23 (11), 1312–1325.

Dhia, B.H., 1998. Problèmes mécaniques multi-échelles: la méthode arlequin. C. R. Acad. Sci. - IIB - Mech.-Phys.-Astron. 326 (12), 899–904.

Dhia, H.B., Rateau, G., 2005. The arlequin method as a flexible engineering design tool. Internat. J. Numer. Methods Engrg. 62 (11), 1442–1462.

Fish, J., Pan, L., Belsky, V., Gomaa, S., 1996. Unstructured multigrid method for shells. Internat. J. Numer. Methods Engrg. 39 (7), 1181–1197.

Flügge, W., 1934. Statik Und Dynamic Der Schalen. Springer-Verlag.

Haryadi, S.G., Kapania, R.K., Haftka, R.T., 1998. Global/local analysis of composite plates with cracks. Composites B 29 (3), 271–276.

Kant, T., Kommineni, J.R., 1994. Large amplitude free vibration analysis of cross-ply composite and sandwich laminates with a refined theory and c° finite elements. Comput. Struct. 50 (1), 123–134.

Kant, T., Owen, D.R.J., Zienkiewicz, O.C., 1982. A refined higher-order c° plate bending element. Comput. Struct. 15 (2), 177–183.

Kirchhoff, G., 1850. Über das gleichgewicht und die bewegung einer elastischen scheibe.. J. Reine Angew. Math. (Crelles J.) 1850 (40), 51–88.

Kubiak, T., Kolakowski, Z., Swiniarski, J., Urbaniak, M., Gliszczynski, A., 2016. Local buckling and post-buckling of composite channel-section beams – numerical and experimental investigations. Composites B 91, 176–188.

Kulikov, G.M., Carrera, E., 2008. Finite deformation higher-order shell models and rigid-body motions. Int. J. Solids Struct. 45 (11), 3153–3172.

Kumar, A., Chakrabarti, A., Bhargava, P., 2013. Vibration of laminated composites and sandwich shells based on higher order zigzag theory. Eng. Struct. 56, 880–888.

Li, G., Carrera, E., Cinefra, M., de Miguel, A.G., Pagani, A., Zappino, E., 2019. An adaptable refinement approach for shell finite element models based on node-dependent kinematics. Compos. Struct. 210, 1–19.

Lindberg, G.M., Olson, M.D., Cowper, G.R., 1969. New developments in the finite element analysis of shells. Quart. Bull. Div. Mech. Eng. Natl. Aeronaut. Establ. 4, 1–38.

Mawenya, A.S., Davies, J.D., 1974. Finite element bending analysis of multilayer plates. Internat. J. Numer. Methods Engrg. 8 (2), 215–225.

Mindlin, R., 1951. Influence of rotary inertia and shear flexural motion of isotropic, elastic plates.. J. Appl. Mech. 18, 31–38.

Murakami, H., 1986. Laminated composite plate theory with improved in-plane responses. J. Appl. Mech. 53, 661–666.

Nguyen, S.-N., L., J., Cho, M., 2015. Efficient higher-order zig-zag theory for viscoelastic laminated composite plates. Int. J. Solids Struct. 62, 174–185.

Noor, A.K., 1986. Global-local methodologies and their application to nonlinear analysis. Finite Elem. Anal. Des. 2 (4), 333–346.

Noor, A.K., Burton, W.S., 1990. Assessment of computational models for multilayered composite shells. Appl. Mech. Rev. 43, 67–97.

Noor, A.K., Mathers, M.D., 1977. Finite element analysis of anisotropic plates. Internat. J. Numer. Methods Engrg. 11 (2), 289–307.

Panda, S.C., Natarajan, R., 1979. Finite element analysis of laminated composite plates. Internat. J. Numer. Methods Engrg. 14 (1), 69–79.

Parisch, H., 1979. A critical survey of the 9-node degenerated shell element with special emphasis on thin shell application and reduced integration. Comput. Methods Appl. Mech. Engrg. 20 (3), 323–350.

Park, K.C., Felippa, C.A., 2000. A variational principle for the formulation of partitioned structural systems. Internat. J. Numer. Methods Engrg. 47 (1–3), 395–418.

Prager, W., 1968. Variational principles for elastic plates with relaxed continuity requirements. Int. J. Solids Struct. 4 (9), 837–844.

Pryor, Jr., C.W., Barker, R.M., 1971. A finite-element analysis including transverse shear effects for applications to laminated plates. AIAA J. 9 (5), 912–917.

Rammerstorfer, F.G., Dorninger, K., Starlinger, A., 1992. Composite and sandwich shells. In: Nonlinear Analysis of Shells By Finite Elements. Springer, pp. 131–194.

Ransom, J.B., 2001. On Multifunctional Collaborative Methods in Engineering Science. National Aeronautics and Space Administration, Langley Research Center.

Reddy, J.N., 1984. A simple higher-order theory for laminated composite plates. J. Appl. Mech. 51, 745–752.

Reddy, J.N., 1989. On computational schemes for global-local stress analysis. In: NASA, Langley Research Center, Computational Methods for Structural Mechanics and Dynamics, Part 1.

Reddy, J.N., 1993. An evaluation of equivalent-single-layer and layerwise theories of composite laminates. Compos. Struct. 25 (1–4), 21–35.

Reddy, J.N., 1997. Mechanics of Laminated Composite Plates and Shells: Theory and Analysis. CRC Press, New York, USA.

Reissner, E., 1945. The effect of transverse shear deformation on the bending of elastic plates. J. Appl. Mech. 12, 69–77.

Reissner, E., Stavsky, Y., 1961. Bending and stretching of certain types of heterogeneous aeolotropic elastic plates. J. Appl. Mech. 28, 402–408.

Szabo, B., Babuška, I., 1991. Finite Element Analysis. John Wiley & Sons.

Zappino, E., Li, G., Pagani, A., Carrera, E., 2017. Global-local analysis of laminated plates by node-dependent kinematic finite elements with variable ESL/LW capabilities. Compos. Struct. 172, 1–14.

Zappino, E., Scano, D., Carrera, E., 2023. Finite element models with node-dependent kinematics based on Legendre polynomials for the global–local analysis of compact and thin walled beams. Comput. Methods Appl. Mech. Engrg. 415, 116212.